Energy levels of the laser active Er^{3+} ion in each of the two crystallographic sites of yttrium orthosilicate

1995 J. Phys.: Condens. Matter 7 5111

(http://iopscience.iop.org/0953-8984/7/26/017)

J. Phys.: Condens. Matter 7 (1995) 5111–5126. Printed in the UK

Energy levels of the laser active Er^{3+} ion in each of the two crystallographic sites of yttrium orthosilicate

J L Doualan†, C Labbé†, P Le Boulanger†, J Margerie†‡, R Moncorgé§ and H Timonen†‖

† Laboratoire de Spectroscopie Atomique, CNRS ERS 137, ISMRA, 14050 Caen Cédex, France
‡ UFR de Sciences, Université de Caen, 14032 Caen Cédex, France
§ Laboratoire de Physico-Chimie des Matériaux Luminescents, CNRS URA 442, Université Lyon I, 69622 Villeurbanne Cédex, France

Received 16 January 1995, in final form 4 April 1995

Abstract. There are two non-equivalent sites of yttrium in the lattice of Y_2SiO_5. Both of them may be occupied substitutionally by Er^{3+}, resulting in a laser active material. We measured absorption spectra of $Y_2SiO_5:Er^{3+}$ at several low temperatures and we studied its emission spectrum at 4.2 K following selective excitation of individual Stark components of the $^4I_{13/2} \rightarrow ^4 I_{15/2}$ transition by the light of a tunable colour centre laser. The results of these two experiments allow classification of the absorption and emission lines into two independent systems, thus yielding two energy level schemes 1 and 2. Moreover, simple crystal field calculations strongly suggest from which Y_2SiO_5 crystallographic site spectrum 1 arises, and from which one spectrum 2.

1. Introduction

Trivalent erbium in various vitreous or crystalline matrices is a very useful laser active ion for amplification or emission in several spectral domains, including the eye safe 1550 nm band ($^4I_{13/2} \rightarrow ^4 I_{15/2}$ transition, see figure 1), of major interest for telecommunications on optical fibres and for ranging applications. Spectroscopic properties of Er^{3+} in yttrium orthosilicate Y_2SiO_5 (we shall write YSO for short) have been investigated by Li *et al* (1992). Room temperature CW laser emission of YSO:Yb^{3+}:Er^{3+} has been achieved at 1576 nm under pumping at 980 nm with a sapphire:Ti^{3+} laser (Li *et al* 1994). Recently, Spariosu *et al* (1994) reported pulsed laser emission of YSO:Er^{3+} at 1633 nm under intracavity pumping by a glass:Er^{3+} laser at 1532 nm. The 1633 nm output was a single giant pulse, which suggests a saturable absorption behaviour of the YSO:Er^{3+} sample. It seems therefore of interest to know accurately the crystal field sublevels of the $^4I_{13/2}$ and $^4I_{15/2}$ states, between which the laser emission takes place, as well as the sublevels of higher states of erbium, terminals of excited state absorptions from $^4I_{13/2}$, which might interfere in the operation of the YSO:Er^{3+} laser.

According to Maksimov *et al* (1970), YSO is a monoclinic crystal (space group C_{2h}^6) with two non-equivalent yttrium sites, both with the lowest (C_1) point symmetry. Table 1 lists for each of them the coordinates of Y^{3+} and of the nearest ions; the notation 'site a', 'site b' defined by this table will be used throughout the present paper. Er^{3+} ions

‖ Permanent address: Department of Physics, University of Joensuu, PO Box 111, 80101 Joensuu, Finland.

0953-8984/95/265111+16$19.50

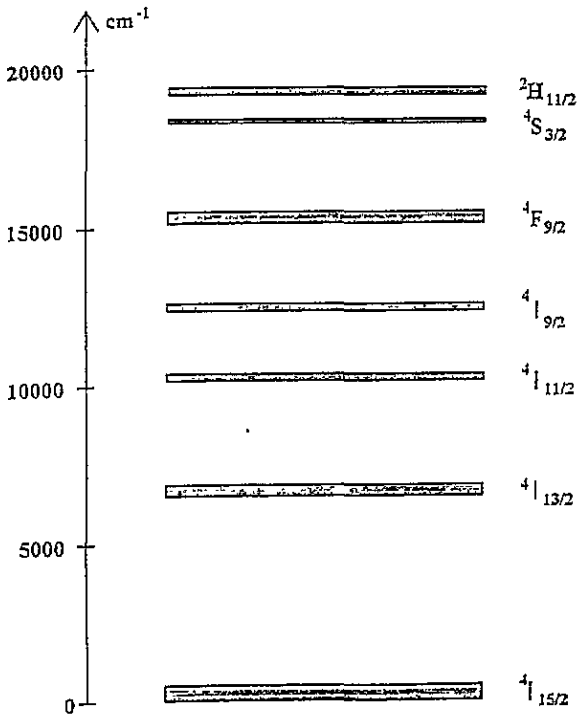

Figure 1. Lowest levels of the Er^{3+} ion.

Table 1. Geometry of the surroundings of Y^{3+} sites a and b in YSO, according to *Structure Reports* (Pearson 1970). The space group is $I2/a$ (C_{2h}^6). Lattice parameters are $a = 10.410$ Å, $b = 6.721$ Å, $c = 12.490$ Å and $\beta = 102°39'$. For each site, the first three columns list the reduced coordinates x/a, y/b, z/c of a neighbouring ion and the last column the distance d in Å of this ion from the central Y^{3+}.

	Site a				Site b			
	x/a	y/b	z/c	d (Å)	x/a	y/b	z/c	d (Å)
Y^{3+}	−0.194	0.378	0.141	0.000	−0.071	−0.257	−0.037	0.000
O^{2-}	−0.382	0.398	0.015	2.231	0.118	−0.398	0.015	2.152
O^{2-}	−0.263	0.429	0.297	2.246	−0.032	−0.343	−0.202	2.261
O^{2-}	−0.118	0.398	−0.015	2.262	−0.054	−0.002	0.089	2.307
O^{2-}	−0.200	0.713	0.118	2.269	0.054	0.002	−0.089	2.348
O^{2-}	−0.237	0.071	0.203	2.282	−0.300	−0.287	−0.118	2.386
O^{2-}	0.032	0.343	0.202	2.321	−0.118	−0.602	−0.015	2.398
O^{2-}	−0.054	−0.002	0.089	3.079	−0.200	−0.287	0.118	2.594
Si^{2+}	−0.127	−0.093	0.181	3.256	−0.127	−0.093	0.181	3.109
O^{2-}	—	—	—	—	−0.263	0.071	−0.203	3.367
Y^{3+}	0.071	0.257	0.037	3.395	0.194	−0.378	−0.141	3.395
				and so on				

(electronic configuration $4f^{11}$) may occupy substitutionally both yttrium sites, with equal or nearly equal probabilities. Thus, an SLJ level of the free ion is split into $(J + \frac{1}{2})$ Kramers doublets for each site, which amounts to $(2J + 1)$ when one takes the two sites

into account. In this context, our main purpose (section 3) is to analyse the absorption and emission spectra of YSO:Er^{3+} in order to classify observed lines into two independent systems and to obtain thus two energy schemes which we shall arbitrarily call '1' and '2'. Then, we shall address ourselves to the question of whether level scheme 1 belongs to crystallographic site a or b (section 4). To the best of our knowledge this latter question has not been studied previously. On the other hand, Li *et al* (1992) have already proposed a system of energy level schemes for each site '1' or '2' in the ground ($^4I_{15/2}$) and the first excited ($^4I_{13/2}$) states. However, our conclusions are completely at variance with theirs about the site assignment of a number of spectral lines, and even, in the case of $^4I_{15/2}$, about the values of the energies of sublevels. The causes of these disagreements will be discussed in section 3.3.

A preliminary account of the present work has been presented at a conference (Doualan *et al* 1994).

2. Experimental methods

We studied two samples of YSO:Er^{3+} prepared by the Czochralski technique at LETI, Grenoble, France. One of them contained 1% and the other 10% molar Er^{3+}. Both were in the shape of platelets, 1.6 mm thick, cut perpendicularly to the crystallographic ⟨010⟩ axis.

We used two home-made helium cryostats, cryostat 1 with the sample clamped on a copper cold finger, cooled by conduction, and cryostat 2 with the sample immersed in the liquid helium bath, and thus more efficiently cooled. For 77 K experiments, we filled the inner vessel of cryostat 1 with liquid nitrogen instead of helium.

Absorption measurements were performed with a Perkin–Elmer Lambda 9 spectrophotometer. For fluorescence experiments, we excited the sample with a home-made CW colour centre laser (CCL). $(F_2^+)_H$ centres in NaCl:OH- (Pinto *et al* 1986) were pumped at 77 K by a Spectron SL 903-2000 YAG:Nd^{3+} laser and permanently reorientated by the blue–green lines of a Coherent Innova 90 Kr^+ laser. A Lyot filter allowed tuning of the CCL emission between 1500 and 1670 nm, but only the short-wavelength part of this spectral domain was useful for the present experiment. The available CCL power was 150 mW, with a spectral width of 1 nm and a horizontal polarization. The sample fluorescence was analysed by a Jobin–Yvon HRS 2 monochromator, equipped with a 600 grooves mm^{-1} grating, and it was received on an ADC 403 liquid-nitrogen-cooled germanium detector. The pumping light was chopped at 125 Hz and the signal from the germanium detector was phase sensitively amplified by a Stanford Research SR 510.

YSO being a biaxial crystal, there are three different spectra (depending on the polarization of light) for electric dipole transitions, and even six spectra (depending on the light propagation direction and on its polarization) for the $^4I_{15/2} \rightarrow {}^4I_{13/2}$ transition which has both forced electric dipole and magnetic dipole characters. However, owing to the very low symmetry of the Er^{3+} surroundings, there are no selection rules and one expects to observe every transition with each polarization (except in the case of an accidentally very small matrix element). Since we are only interested in the level positions, we performed no systematic study as a function of light polarization. In all experiments, the samples had their so-called D_1 axis (Li *et al* 1992) horizontal, so that the fluorescence in section 3.2 was excited with polarization D_1. The fluorescence was studied in a mixture of D_1 and D_2 polarizations, as well as the absorption in section 3.3. However, in both cases, the relative weights of D_1 and D_2 lights were different from 1:1 because of the partial polarization introduced by the diffraction gratings.

The Perkin–Elmer spectrophotometer and the Jobin–Yvon monochromator yield

Table 2. Energies (in cm^{-1}) of the Stark sublevels, up to 20 000 cm^{-1}, of YSO:Er^{3+} at 4.2 K for sites 1 (column 3) and 2 (column 7). Letters r (resonance line), f (fluorescence) and a (absorption) indicate that assignment has been obtained from sections 3.1, 3.2 and 3.3 respectively. A question mark signals an uncertain assignment. For $^2H_{11/2}$, we were unable to classify, even tentatively, the observed levels 19 142 and 19 228 cm^{-1}. Columns 5 and 9 contain for comparison the data from Li *et al* (1992) and Li (1992), divided by the air refraction index 1.000 275. For $^4I_{13/2}$, *(1) or (2) indicates an assignment opposite to ours; for higher levels, (u) means unidentified.* The data of Li *et al* (1992) for $^4I_{15/2}$ have not been included in this table since most of them have no relationship at all with ours (see section 3.3).

		Site 1				Site 2			
		This work		Li *et al* (1992) Li (1992)		This work		Li *et al* (1992) Li (1992)	
$^4I_{15/2}$	1	0				0			
	2	42	f, a			28	f, a		
	3	86	f, a			63	f, a		
	4	104	f, a			128	f, a		
	5	172	f, a			169	f, a		
	6	424?	f			314	f		
	7	481	f			350	f		
	8	513	f			415	f		
$^4I_{13/2}$				6469.5					
	1	6507	r, f	6508		6497	r, f	6497.5	
								6538	
	2	6547	f, a	6549		6563	f, a	6564	
	3	6596.5	f, a	6596		6592	f, a		
	4	6623	f, a	6623	(2)	6621	f, a		
				6773					
	5	6798	a			6725	a	6726	(1)
	6	6852	a	6852		6750	a	6750	
	7	6871	a	6871	(2)	6798	a	6799	
$^4I_{11/2}$	1	10 193	a	10 195.0	(u)	10 179	a	10 180.4	(u)
	2	10 271?	a	10 272.5	(u)	10 193?	a	10 195.0	(u)
	3	10 292?	a	10 295.8	(u)	10 232.5	a	10 234.7	(u)
	4	10 308?	a	10 312.8	(u)	10 250	a	10 252.5	(u)
				10 348.0	(u)				
	5	10 369	a	10 370.5	(u)	10 308?	a	10 312.8	(u)
	6	10 383?	a	10 386.7	(u)	10 341	a	10 342.7	(u)
$^4I_{9/2}$	1	12 359.5	a	12 362.1	(u)	12 376	a	12 382.0	(u)
	2	12 459.5?	a	12 456.1	(u)	12 448	a		
	3	12 527.5?	a	12 527.9	(u)	12 492?	a	12 493.4	(u)
	4	12 612	a	12 610.0	(u)	12 563	a	12 565.6	(u)
	5	12 649.5	a	12 651.5	(u)	12 605	a	12 610.0	(u)
$^4F_{9/2}$	1	15 169	a	15 170.3	(u)	15 195.5	a	15 197.9	(u)
	2	15 220.5	a	15 221.1	(u)	15 220.5	a	15 221.1	(u)
	3	15 360.5?	a	15 361.5	(u)	15 303	a	15 305.0	(u)
	4	15 381.5	a	15 380.4	(u)	15 381.5?	a	15 380.4	(u)
	5	15 498	a	15 499.5	(u)	15 424.5	a	15 427.8	(u)
$^4S_{3/2}$	1	18 267	a	18 269.8	(u)	18 308	a	18 310.0	(u)
	2	18 372	a	18 373.8	(u)	18 417	a	18 417.8	(u)
$^2H_{11/2}$		19 091	a	19 093.2	(u)	19 070	a	19 071.4	(u)
		19 166 ?	a	19 166.4	(u)	19 132	a	19 137.1	(u)
		19 315	a	19 314.6	(u)	19 159?	a		
						19 201	a	19 203.3	(u)
						19 244?	a	19 247.6	(u)
						19 266	a	19 269.9	(u)

wavelengths in air. However, throughout this paper, we describe our results in terms of vacuum wavelengths (and vacuum wavenumbers). The correction is of the same order of magnitude as experimental uncertainties on line positions (section 3.4). Therefore, it is pointless to take into account the dispersion of the air refraction index and, in the calculation of the air to vacuum correction, we assume this index to be 1.000 275 in the whole investigated spectral domain.

3. Experimental results

When switching from the 1% to the 10% erbium-doped sample, we observed the absorption and emission lines intensities to increase by a factor of the order of 10, but no new lines appeared, which shows that no transitions due to pairs of erbium ions arise with sizeable intensity, even in the more concentrated sample.

The classification of spectral lines into two systems 1 and 2 and the building up of the corresponding level schemes proceeded in three stages (subsections 3.1, 3.2 and 3.3 below). A final subsection 3.4 will contain a brief discussion of experimental results.

3.1. The resonance lines

For the $^4I_{15/2} \rightarrow {}^4 I_{13/2}$ transition in the near infrared, two and only two lines appear both in absorption and in emission at 4.2 K: G and H (1536.7 and 1539.2 nm respectively, see figures 2 and 3). They obviously connect, for the two crystalline sites, the lowest Stark sublevel of $^4I_{15/2}$ (at 0.0 cm^{-1}) and the lowest Stark sublevel of $^4I_{13/2}$. Thus, we locate the sublevel $^4I_{13/2}$ (1) at 6507 cm^{-1} for one site which we shall arbitrarily call 'site 1' and at 6497 cm^{-1} for the other site or 'site 2'.

3.2. Selectively excited fluorescence spectra

With the 10% concentrated sample, the fluorescence spectrum at 4.2 K is observed to be exactly the same, whatever the choice of the excitation line. Obviously, during the long lifetime (4.7 ms) of $^4I_{13/2}$ an efficient exchange of excitation takes place between ions in sites 1 and 2 and one observes the emission of both sites with comparable intensities.

On the other hand, figure 3 shows that with the 1% doped sample, the 4.2 K fluorescence spectrum is very different following 1527 or 1524 nm (F or E) excitation. In the latter case, the spectrum is 'pure', it consists only of 8 lines, with wavelengths λ_i ($i = 1, 2, \ldots, 8$), among which is the resonance transition H, 1539 nm (section 3.1). This proves that absorption line E, 1524 nm, belongs to system 2 and strongly suggests that the eight lines of figure 3(b) correspond, for site 2, to the transitions from the lowest Stark sublevel of $^4I_{13/2}$ to the eight sublevels of $^4I_{15/2}$. In table 2, we list the energies of these sublevels calculated by

$$E_i \ (\mathrm{cm}^{-1}) = 6497 - 1/\lambda_i. \tag{1}$$

With excitation by F, 1527 nm, (figure 3(a)), the spectrum is somewhat more complicated: it contains, but with much reduced intensity, the lines which were already present in figure 3(b) in addition to entirely new ones, among which is the other resonance transition G, 1537 nm. The latter fact indicates that the absorption line F belongs to system 1, as well as those fluorescence lines which appear in figure 3(a), but not in figure 3(b). The presence, with a weak intensity, of fluorescence lines pertaining to system 2 in the spectrum 3(a) shows that, following F excitation, sublevel 1 of $^4I_{13/2}$ of site 2 is feebly populated,

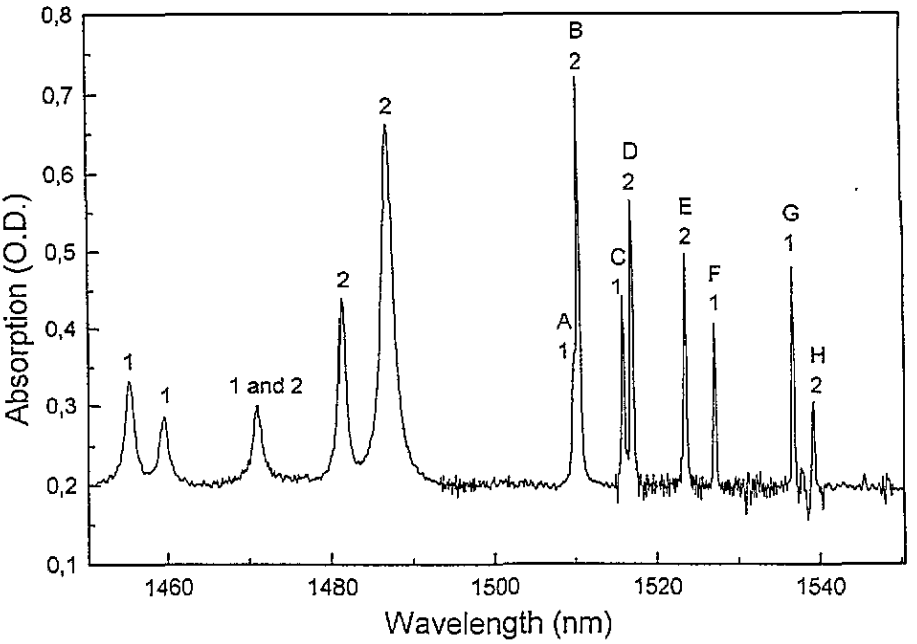

Figure 2. Absorption spectrum of 1% erbium-doped YSO at ~7 K. Number 1 or 2 above a line indicates the spectrum to which it pertains according to sections 3.1, 3.2 and 3.3. The longest-wavelength lines are also labelled A, B,..., H, in order to facilitate the reading of section 3.

in addition to the preferentially populated homologous sublevel of site 1. This has most probably an instrumental origin, such as a spectral overlapping of the CCL emission with the wing of an absorption line belonging to system 2. This slight 'contamination' of the spectrum of figure 3(a) does not prevent us from calculating the energies E_i of the $^4I_{15/2}$ Stark sublevels of site 1 by the formula:

$$E_i \ (\mathrm{cm}^{-1}) = 6507 - 1/\lambda_i' \tag{2}$$

where the λ_i' are the new wavelengths of figure 3(a). The results are listed in the third column of table 2. However, spectrum 3(a) contains only six 'new' lines instead of the eight which are expected. Where are the two remaining $^4I_{15/2}$ sublevels for site 1? One of them is easily found by remarking that line I near 1546 nm is strong in both spectra 3(a) and 3(b) and that, on closer examination, its location is slightly different (1546.0 and 1546.7 nm following E and F excitation respectively), which allows us to locate the second Stark sublevel of $^4I_{15/2}$ at 42 cm^{-1} for site 1. The last component may be found from figure 4 which shows with an increased sensitivity the long-wavelength part of figure 3. In spectrum 4(a), the 'parasitic' lines 1617, 1627 and 1644 nm are nearly as intense as the 'new' lines 1659 and 1668 nm which belong to site 1. But their relative intensities are 1.00: 0.45: 1.00, to be compared with 1.00: 0.45: 0.44 in the site 2 pure spectrum of figure 4(b) (do not attempt to compare directly figures 4(a) and 4(b), their ordinate scales are different). Thus the 1644 nm emission line may be a mixture of two components, one pertaining to site 2, as is evident from figure 4(b), and the other to site 1, as is suggested by its significant relative intensity increase in figure 4(a). This is however indirect evidence, so that the corresponding 424 cm^{-1} sublevel of site 1 is considered as only tentative.

Experiments similar to the ones of figure 3 have also been performed with the exciting

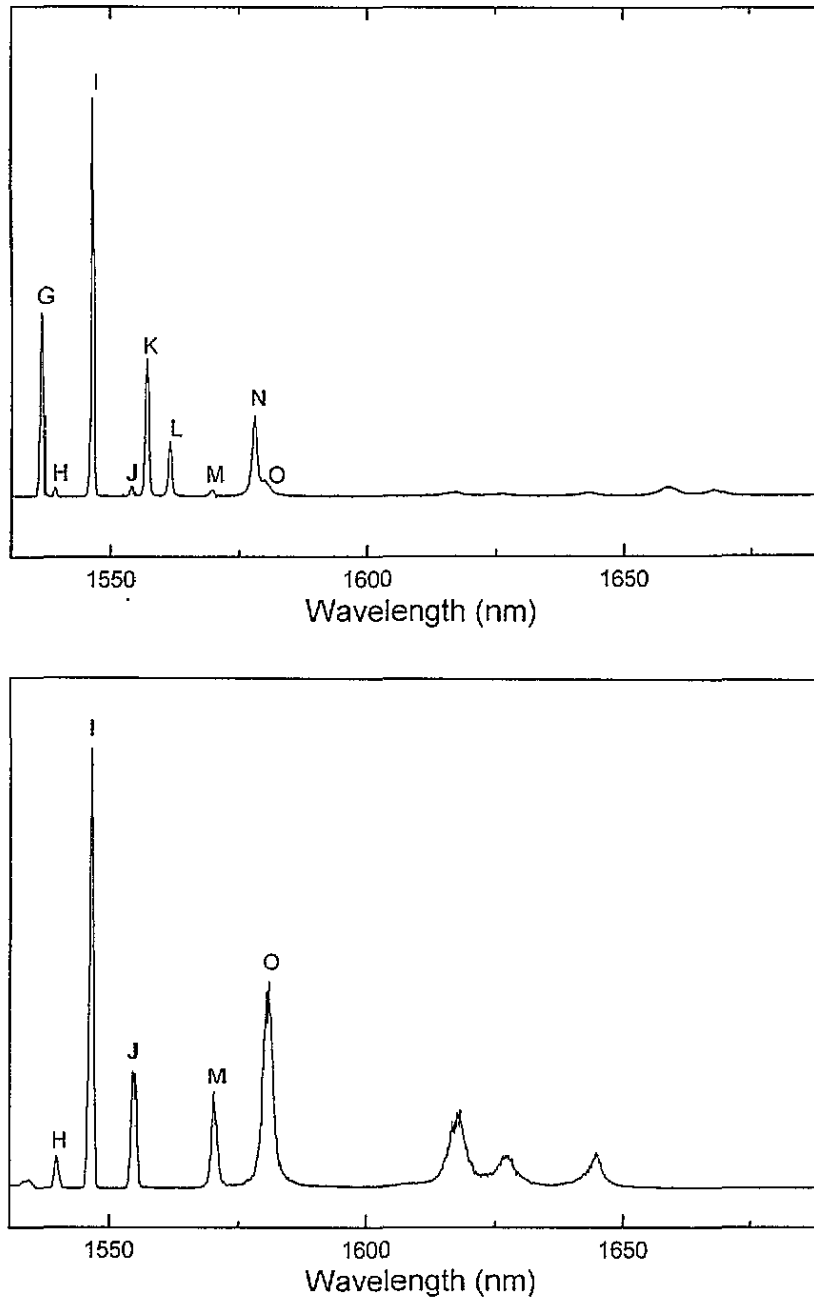

Figure 3. Emission spectra of 1% erbium-doped YSO at 4.2 K: (a) excitation at 1527 nm; (b) excitation at 1524 nm. The ordinate scale is arbitrary and different for the two spectra. The shortest-wavelength lines are labelled G, H,..., O, in order to facilitate the reading of section 3.

laser tuned at 1537 or 1510.4 nm (lines G and B of figure 2). We obtained results similar in the former case to figure 3(a) and in the latter to figure 3(b), which confirms that excited level 6507 cm^{-1} belongs to site 1 and attributes level 6621 cm^{-1} to site 2.

We also measured excitation spectra: setting the HRS 2 monochromator on the long-

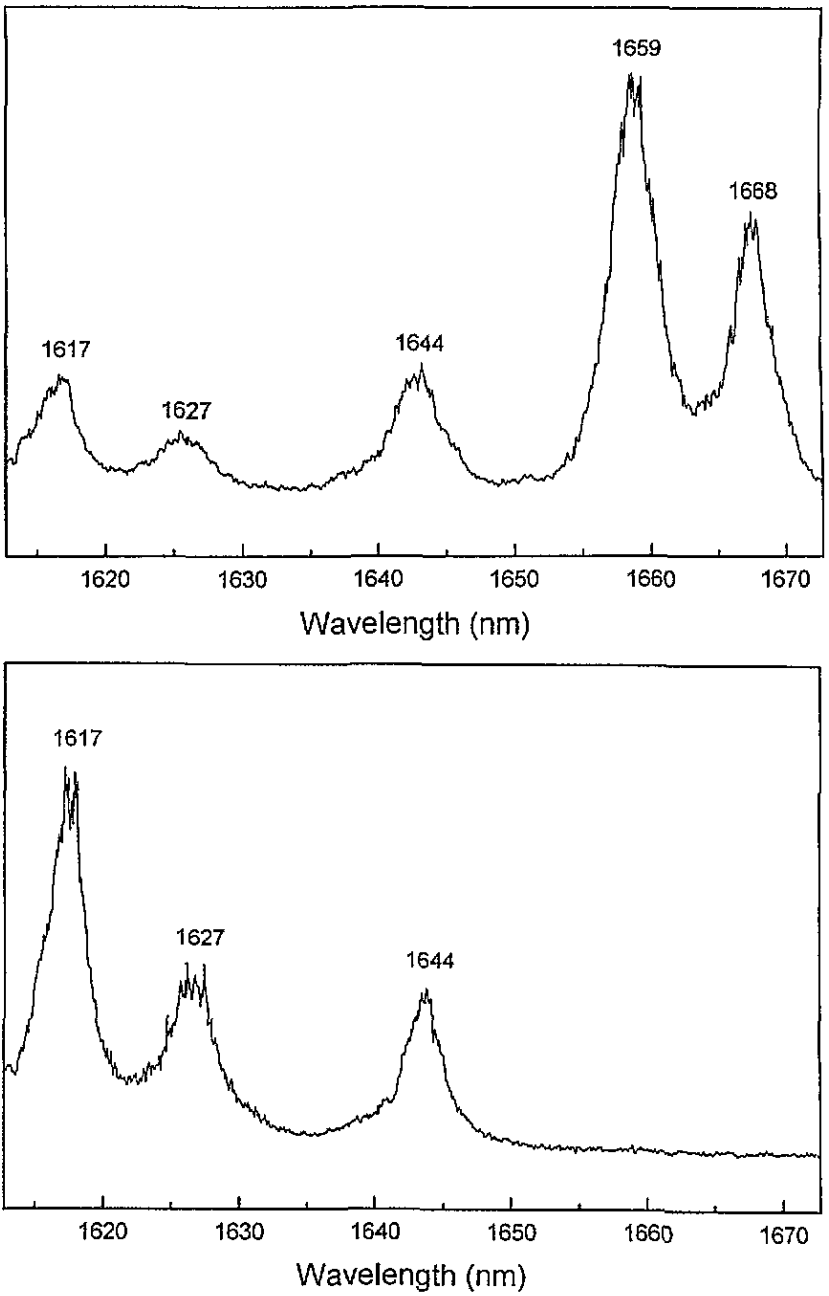

Figure 4. Same as figure 3, but in a smaller spectral domain and with an increased sensitivity. Each emission peak is labelled by its wavelength in nanometres.

wavelength wing of the I (1546 nm) complex discussed above, we swept the CCL wavelength by motor rotating its Lyot filter. We thus registered an excitation spectrum with only four lines in the explored domain ($\lambda > 1500$ nm): A, C, F and G (1509.9, 1516, 1527 and 1537 nm), which confirmed once again that levels 6507 and 6547 cm^{-1} belong to site 1 and added two new excited levels to this list: 6596.5 and 6623 cm^{-1}. Setting the monochromator

on the other side of the I group, we registered an excitation spectrum with seven lines: D, E and H (1517, 1524 and 1539 nm) in addition to the four lines previously mentioned. Obviously, the monochromator was not so cleverly tuned as in the previous experiment, it selected a mixture of the 1546.7 and 1546.0 fluorescence lines (belonging to sites 1 and 2 respectively). However, this experiment shows unambiguously that the additional excitation lines (D, E and H) belong to site 2. This was already known for the two last lines, but the first one adds a new sublevel (6592 cm^{-1}) to our list for site 2.

3.3. Absorption spectra

We could not go further with the method of section 3.2 for lack of tunability of our CCL towards shorter wavelengths. Therefore, we sought the missing information by a study of the absorption spectrum as a function of temperature. From the energies of $^4I_{15/2}$ sublevels (table 2), one calculates their populations for thermal equilibrium at different temperatures (table 3). At 4.2 K sublevels 1 of both sites are the only ones to be significantly populated (as we tacitly assumed in the two previous subsections), but at temperatures as low as 10 K the population of sublevel 2 of site 2 is no longer negligible, so that one expects to observe 'hot' satellites at 28 cm^{-1} to the red of the main ('cold') absorption lines for site 2. This was indeed the chief cause of the erroneous identifications of Li *et al* (1992): since the temperature of their sample was ~10 K, they mistook a number of these hot satellites for main lines, hence their extra 'sublevels' 6469.5, 6538 and 6773 cm^{-1} (columns 5 and 9 of table 2). The most detrimental error concerned the 6469.5 cm^{-1} (i.e. I or 1546 nm) transition, $^4I_{15/2}$ (2) $\rightarrow{}^4I_{13/2}$ (1), which of course appears also in the very-low-temperature emission spectrum and was therefore mistaken as one of the resonance lines. Thus, Li *et al* considered 1546 and 1539 nm as the two resonance lines, instead of 1537 and 1539 nm. Since the resonance lines are the cornerstone of the whole site assignment process, everything went wrong after this initial error and a number of Li *et al*'s energies of $^4I_{15/2}$ sublevels were completely false since they were calculated from $6469.5 - 1/\lambda_i'$ instead of equation (2). This emphasizes how important it is to perform the experiments of sections 3.1 and 3.2 with the sample really at 4.2 K, and not at some slightly higher temperature.

Table 3. Populations (in %) of the $^4I_{15/2}$ ground state sublevels at thermal equilibrium.

	4.2 K		10 K		77 K	
Sublevel	Site 1	Site 2	Site 1	Site 2	Site 1	Site 2
1	100.00	99.99	99.76	98.24	54.33	49.03
2	0.00	0.01	0.24	1.75	24.78	29.06
3	0.00	0.00	0.00	0.01	10.89	15.11
4	0.00	0.00	0.00	0.00	7.78	4.49
5	0.00	0.00	0.00	0.00	2.18	2.08
6	0.00	0.00	0.00	0.00	0.02	0.14
7	0.00	0.00	0.00	0.00	0.01	0.07
8	0.00	0.00	0.00	0.00	0.01	0.02

But once the list of the 4.2 K absorption and emission lines has been safely established, absorption experiments at higher temperatures provide valuable clues concerning the site identifications. With our helium cryostat 1 (section 2), the real temperature of the sample was probably ~10 K since extra (hot) absorption lines appeared, which were completely absent when the same sample was studied in the more efficient cryostat 2. The intensity of these

hot lines changed randomly from an experiment to the next, probably as a consequence of the sample being fixed in more or less close contact with the cold finger. In all cases, the hot lines observed with cryostat 1 filled with liquid helium were found to be at 28 cm^{-1} to the red of some main line, which allowed us to associate with site 2 a number of absorption transitions, not only toward $^4I_{13/2}$, but also toward more excited states $^4I_{11/2}, ^4I_{9/2}, \ldots, ^2H_{11/2}$ (see table 2).

Table 4. Achievements and shortcomings of site determination from absorption spectra.

	$^4I_{13/2}$	$^4I_{11/2}$	$^4I_{9/2}$	$^4F_{9/2}$	$^4S_{3/2}$	$^2H_{11/2}$
Number of expected sublevels	14	12	10	10	4	12
Number of observed absorption lines at 4.2 K	13	10	10	8	4	11
Number of uncertain assignments	0	6	3	2	0	3
Number of completely unidentified sublevels	0	0	0	0	0	3
Average interval between sublevels (cm^{-1})	29	19	32	37	50	22
Instrumental resolution (nm)	~0.7	~0.7	0.2	0.2	0.1	0.1
Instrumental resolution (cm^{-1})	~3	~7	3	5	3	4
Accuracy of wavenumber determination (cm^{-1})	3.5	8	3	5	7	7

To proceed further, we use absorption spectra at 77 K. From table 3, one remarks that in both sites one expects to observe with a large intensity hot satellites arising from ground state sublevels 2 and 3 and with quite detectable intensities from sublevels 4 and 5. For site 1 these satellites should sit at 42, 86, 104 and 172 cm^{-1} to the red of the main line and for site 2 at 28, 63, 128 and 169 cm^{-1} (table 2). Indeed, each of these ground state intervals has been unambiguously observed for the 77 K satellites of several main lines. The trouble is that the resolution of absorption spectra is too bad (table 4) to allow full resolution of the great number of lines which arise at 77 K. The weaker satellites at 104, 128, 169 and 172 cm^{-1} could only be observed for the one or two main lines with the longest wavelengths in each SLJ multiplet, i.e. when they are situated in spectral regions with no overlapping with stronger lines. Therefore, most of the identification work was performed with the help of the 28, 42, 63 and 86 cm^{-1} satellites. The results are listed in columns 3 and 7 of table 2. Question marks indicate sublevels for which the attribution to site 1 or 2 is uncertain. This can happen for one of the following reasons:

(i) Only one hot satellite, (s), suggests a particular assignment for main line (m), but (s) can also be interpreted as being one of the hot satellites of some other main line (m′), within the measurement accuracy, which is limited by the instrumental resolution (table 4) and, for some absorption lines, by their intrinsic width.

(ii) Neither the first, nor the second hot satellite is observed for a particular main line (m), but another main line (M) is situated at approximately 42 (or 28) cm^{-1} on the red side of (m), so that (m) may belong to site 1 (or to site 2), with its first hot satellite unresolved from main line (M).

(iii) Some main line (m) is suspected to be a blend of two transitions (m_1) and (m_2), one from each site, but conclusive evidence is lacking for one of these sites (or for both) because of one of the factors (i) or (ii).

In view of the above problems, the site assignment of the sublevels of a given SLJ state is all the more easy and safe where: the optical absorption is intense (thus allowing a good signal to noise ratio with narrow slits for the spectrophotometer), J is small (not too many sublevels to classify) and the average crystal field splitting is large (thus limiting

the degree of overlapping between spectral lines), the wavelength is long (so that a given wavelength resolution should correspond to a better wavenumber resolution). Table 4 shows to what extent these various requirements are fulfilled for the levels we have studied. In particular, it is very easy to classify the sublevels of $^4S_{3/2}$ because of their small number and large splittings, while we could reach only incomplete and uncertain conclusions for $^4I_{11/2}$ (small splittings and very weak absorption) as well as for $^2H_{11/2}$ (small splittings and short wavelength). In view of the shortcomings met in the latter case, we thought it useless to attempt an analysis of still higher-lying states.

3.4. Discussion

The uncertainty on wavenumbers of the sublevels of SLJ excited states in columns 3 and 7 of table 2 is due to the limited accuracy of the wavelength scale of the Lambda 9 spectrophotometer: 0.2 nm below 861 nm and 0.8 nm above, according to the manufacturer. The corresponding wavenumber uncertainty for each SLJ state is indicated in the last line of table 4. The reproducibility of our experimental data has been observed to be significantly higher, and, therefore, the internal consistency of results is better than the absolute values of wavelengths or wavenumbers.

The $^4I_{15/2}$ ground state intervals were derived from the fluorescence experiments (formulae (1) and (2) of section 3.2), even though the location of sublevels 2–5 for each site was independently verified by absorption measurements (section 3.3). The important point here is therefore the irreproducibilities in our measurements of the positions of the different lines on the HRS 2 monochromator wavelength scale, rather than the absolute accuracy of this scale itself. From the dispersion of results, the uncertainty on the final result is estimated to be 1 cm^{-1} for sublevels 2–5 and 2 cm^{-1} for levels 6–8 which are known only through broader and weaker lines.

With the wavenumbers of table 2, we calculate the spectral locations of all components of transitions $^4I_{13/2} \rightarrow^4 I_{15/2}$ and $^4I_{13/2} \rightarrow^4 I_{9/2}$ which may be observed respectively in emission and in excited state absorption at room temperature (assuming a negligible temperature shift of erbium levels). We thus tentatively conclude that the lasing transition in the case of Li *et al* (1994) was $^4I_{13/2}$ (6) $\rightarrow^4 I_{15/2}$ (8) of site 1 (calculated wavelength 1577.5 nm, versus 1576 observed) or perhaps a superposition of $^4I_{13/2}$ (1) $\rightarrow^4 I_{15/2}$ (5) of site 1 and of $^4I_{13/2}$ (6) $\rightarrow^4 I_{15/2}$ (8) of site 2 (both calculated at 1578.5 nm). For the laser of Spariosu *et al* (1994), the most plausible assignment is the transition $^4I_{13/2}$ (2) $\rightarrow^4 I_{15/2}$ (6) of site 1 which is calculated exactly at the observed wavelength, 1633 nm (two other transitions are expected to lie respectively 2 and 3 nm farther on the long wavelength side). The giant pulse behaviour of Spariosu *et al* 's laser suggests that the active sample could also play the role of a saturable absorber. From our results, it seems dubious that absorption in the $^4I_{13/2}$ excited state could be involved: the nearest calculated component of $^4I_{13/2} \rightarrow^4 I_{9/2}$ is at 1637 nm, i.e. 4 nm from the laser emission. In order to get more conclusive information on this point, we are currently measuring directly the room-temperature absorption spectrum of the $^4I_{13/2}$ level of YSO:Er^{3+}. We hope to be soon able to report about this new experiment.

4. Crystal field calculations

The aim of the present section is not to make an elaborate theoretical study of the spectrum of YSO:Er^{3+} (like, for instance, the one of Gruber *et al* (1993) concerning erbium-doped garnets), but to perform the simplest calculation which will be able to answer unambiguously to the following question: does spectrum 1, as determined in section 3, correspond to

crystallographic site a or b (section 1)? We shall describe below the model we have chosen (subsection 4.1), then the calculations and their results (subsection 4.2).

4.1. Model

The crystal field potential V_c acting on the rare-earth ion, situated at the origin of coordinates, may be written as (see for instance Judd 1963)

$$V_c = \sum_{i,k,q} B_k^q \, r_i^k \, Y_{kq}(\theta_i, \varphi_i) \tag{3}$$

where i labels the optical electrons with spherical coordinates $(r_i, \theta_i, \varphi_i)$, Y_{kq} is a spherical harmonic and the B_k^q are coefficients. Other authors use slightly different notations. For instance, Wybourne's (1965) B_q^k is Judd's (or our) B_k^q multiplied by $\sqrt{(2k+1)/4\pi}\,\langle r^k \rangle$, where $\langle r^k \rangle$ is the average value of r^k for a 4f electron. In the case of an incomplete f shell, k is limited to even values, smaller than or equal to six. The term $k = 0$ shifts the whole $4f^n$ configuration by the same amount, it is therefore omitted and the summation is thus limited to terms with $k = 2, 4$ and 6. In many cases, the number of values of q, too, is strongly limited thanks to point symmetry arguments. But here the symmetry group is C_1 and all the values of q must be retained, so that we have $5 + 9 + 13 = 27$ B_k^q coefficients for each of the two erbium sites. Thus, the standard procedure of considering the B_k^q as adjustable parameters is hopeless. Moreover, it would be of no interest since our aim is precisely to distinguish between the two possible sites, using the relationship between their geometry and their crystal field potential. We therefore turn to the very naïve model in which ligand ions are considered as mere fixed point charges of value $-g_j e$, with spherical coordinates $(\rho_j, \alpha_j, \beta_j)$. One thus obtains from the spherical harmonics addition theorem (Judd 1963, equation 2-3):

$$B_k^q = \frac{1}{(2k+1)\varepsilon_0} \sum_j \frac{g_j e^2}{\rho_j^{k+1}} \, Y_{kq}^*(\alpha_j, \beta_j). \tag{4}$$

Of course, it was recognized long ago that formula (4) yields values of B_k^q in complete disagreement with those obtained by a parametric fit of observed spectra. However, Judd (1957) remarked that, in the case of $LaCl_3$:Pr^{3+} (with only four non-zero B_k^q coefficients i.e. B_2^0, B_4^0, B_6^0 and B_6^6), the B_6^6/B_6^0 ratio predicted by formula (4) can be used safely. We tentatively generalize this result by postulating that formula (4), which cannot cope with radial aspects of crystal potential is fully able to describe its angular properties. Practically, it means that all the B_k^q coefficients we need will be calculated from the geometry of the relevant site (a or b) through formula (4), except that we shall introduce an adjustable multiplicative factor, with three independent values for $k = 2, 4$ or 6. This hypothesis amounts to considering the average values $\langle r^2 \rangle$, $\langle r^4 \rangle$ and $\langle r^6 \rangle$ for a 4f electron as three adjustable parameters, with physically meaningless values.

A second point will be to choose the geometry of the cluster of j ions in the summation of equation (4). There is an ambiguity in the structural results of Maksimov *et al* (1970), as pointed out by *Structure Reports* (Pearson 1970): in order to obtain a better agreement with interatomic distances quoted by the former reference, the authors of *Structure Reports* have shifted the origin by subtracting $0.25a$ from all x coordinates given in table 2 of Maksimov *et al* , while leaving y and z coordinates unaltered. Because of the operations of the crystal space group, this abscissa modification is by no means innocent; it modifies the distances and angles for most ions. We chose to adhere to the hypothesis of *Structure Reports* and, in order to prevent any misunderstanding, we give explicitly in table 1 the

resulting coordinates for all ions of interest. Of course, the input data of the crystal field calculations of section 4.2 will have to be modified if the real geometry of ions in YSO is subsequently found to differ from the one of *Structure Reports* (Pearson 1970).

We must then decide which neighbours j we include in the summation (4). The effect of distant ions is expected to be shielded by nearer ones. Thus, in order to make the calculation both simple and reliable, one should consider only the anions in the first coordination shell of the active ion. One sees in table 1 that, in both sites, the first neighbours are a group of six oxygens ~2.2–2.3 Å from the erbium ion. Then comes a seventh oxygen, somewhat more distant, then a silicon, then other ions with the order of increasing distances differing in sites a and b. Thus, we may hesitate whether to include the six or the seven nearest oxygens in the expression of V_c. Finally, we performed successively the whole calculation of section 4.2 in both hypotheses, with rather similar final results (except for the physically meaningless numerical values of the $\langle r^k \rangle$ parameters). Thus we only report below the results obtained when taking into account, in each Er^{3+} site, the seven nearest oxygens (of charge $g_j = 2$).

A third simplifying assumption will be to use for $^4I_{15/2}$ and $^4I_{13/2}$ pure *LS* coupling wavefunctions. Of course, one knows that intermediate coupling plays an important role in rare-earth ion spectra. However, there are only three levels with $J = \frac{15}{2}$ and also three with $J = \frac{13}{2}$ in the $4f^{11}$ configuration. $^2L_{15/2}$ and $^2K_{15/2}$ lie more than 25 000 cm^{-1} above $^4I_{15/2}$; $^2K_{13/2}$ and $^2I_{13/2}$ also more than 25 000 cm^{-1} above $^4I_{13/2}$, so that $^4I_{15/2}$ and $^4I_{13/2}$ may be expected to have fairly pure *LS* coupling wavefunctions. This is confirmed in the case of $LaCl_3$:Er^{3+} by Rajnak (1965) who calculates purities of 97.1% and 99.1% for $^4I_{15/2}$ and $^4I_{13/2}$ respectively. On the other hand, we shall not attempt to include in our crystal field calculations $^4I_{11/2}$, $^4I_{9/2}$, $^4F_{9/2}$, $^4S_{3/2}$ and $^2H_{11/2}$, the wavefunctions of which are really mixtures of several *SLJ* levels. This restriction of the domain of our study is immaterial since the consideration of $^4I_{15/2}$ and $^4I_{13/2}$ will provide us with enough information to differentiate between the two crystallographic sites.

Our last approximation will be to neglect the effect of off-diagonal V_c matrix elements between $^4I_{15/2}$ and $^4I_{13/2}$. This should be valid since the distance between these levels (~6500 cm^{-1}) is noticeably larger than their crystal field splittings (~500 cm^{-1}).

4.2. Calculations and results

Following Wybourne (1965), we introduce the multielectronic unit tensor operator $\mathbf{U}^{(k)}$ and the monoelectronic tensor operator $\mathbf{C}^{(k)}$:

$$\mathbf{C}_q^{(k)} = \sqrt{\frac{4\pi}{2k+1}}\, Y_{kq}(\theta, \varphi). \tag{5}$$

Then, in analogy with Wybourne's equation (6-3):

$$\langle {}^4I_J, M | \sum_i r_i^k\, Y_{kq}(\theta_i, \varphi_i) | {}^4I_J, M' \rangle$$

$$= \sqrt{\frac{2k+1}{4\pi}}\, \langle r^k \rangle\, \langle \ell \,\|\mathbf{C}^{(k)}\|\, \ell \rangle\, \langle {}^4I_J, M\, |\mathbf{U}_q^{(k)}|\, {}^4I_J, M' \rangle \tag{6}$$

where $\ell = 3$ is the monoelectronic orbital angular momentum quantum number and $\langle r^k \rangle$ is one of the three adjustable parameters discussed above. According to Wybourne's (1965) equation (2-37), the reduced matrix element of $\mathbf{C}^{(k)}$ is:

$$\langle \ell \,\|\mathbf{C}^{(k)}\|\, \ell \rangle = (-1)^\ell\, (2\ell+1) \begin{pmatrix} \ell & k & \ell \\ 0 & 0 & 0 \end{pmatrix} \tag{7}$$

where

$$\begin{pmatrix} \ell & k & \ell \\ 0 & 0 & 0 \end{pmatrix}$$

is a $3j$ symbol. The Wigner–Eckart theorem yields

$$\langle {}^4\mathrm{I}_J, M \left| U_q^{(k)} \right| {}^4\mathrm{I}_J, M' \rangle = (-1)^{J-M} \begin{pmatrix} J & k & J \\ -M & q & M' \end{pmatrix} \langle {}^4\mathrm{I}_J \left\| \mathbf{U}^{(k)} \right\| {}^4\mathrm{I}_J \rangle \quad (8)$$

where

$$\begin{pmatrix} J & k & J \\ -M & q & M' \end{pmatrix}$$

is again a $3j$ symbol. From standard tensorial operator methods (Judd 1963, equation (3-38))

$$\langle {}^4\mathrm{I}_J \left\| \mathbf{U}^{(k)} \right\| {}^4\mathrm{I}_J \rangle = (-1)^{3/2+6+J+k} (2J+1) \begin{Bmatrix} J & k & J \\ 6 & \frac{3}{2} & 6 \end{Bmatrix} \langle {}^4I \left\| \mathbf{U}^{(k)} \right\| {}^4I \rangle \quad (9)$$

where

$$\begin{Bmatrix} J & k & J \\ 6 & \frac{3}{2} & 6 \end{Bmatrix}$$

is a $6j$ symbol and the reduced matrix elements $\langle {}^4I \left\| \mathbf{U}^{(k)} \right\| {}^4I \rangle$ are tabulated by Nielson and Koster (1963). We read in their table the values for the $4f^3$ configuration and we change the signs because

$$\langle \alpha SL \left\| \mathbf{U}^{(k)}(4\ell + 2 - n) \right\| \alpha' S'L' \rangle = -(-1)^k \langle \alpha SL \left\| \mathbf{U}^{(k)}(n) \right\| \alpha' S'L' \rangle. \quad (10)$$

From formulae (3), (4) and (6) to (10), we build the four perturbation matrices $\mathcal{V}_c$, with elements $\langle s, {}^4\mathrm{I}_J, M | V_c | s, {}^4\mathrm{I}_J, M' \rangle$, for $J = \frac{15}{2}$ or $\frac{13}{2}$ and for the site s equal to a or b. In this calculation, we use the crystallographic data for YSO as given in table 1. The $\mathcal{V}_c$ matrices have complex elements with the symmetry properties

$$\langle s, {}^4\mathrm{I}_J, M | V_c | s, {}^4\mathrm{I}_J, M' \rangle = \left[\langle s, {}^4\mathrm{I}_J, M' | V_c | s, {}^4\mathrm{I}_J, M \rangle \right]^* \quad (11)$$

(Hermiticity of operator V_c) and

$$\langle s, {}^4\mathrm{I}_J, M | V_c | s, {}^4\mathrm{I}_J, M' \rangle = (-1)^{M-M'} \left[\langle s, {}^4\mathrm{I}_J, -M | V_c | s, {}^4\mathrm{I}_J, -M' \rangle \right]^* \quad (12)$$

which is a consequence of equations (3), (4), (6) and (8) and which ensures Kramers degeneracy of levels. The four $\mathcal{V}_c$ matrices are diagonalized and their eigenvalues are compared with experimental data. Since V_c has been written without $k = 0$ contribution, the trace of each $\mathcal{V}_c$ matrix vanishes and therefore the sum of its eigenvalues is automatically zero. This is taken into account in the fitting procedure: for each group of experimental data in table 2 ($^4\mathrm{I}_{15/2}$ or $^4\mathrm{I}_{13/2}$; site 1 or site 2), the wavenumber origin is shifted to the centre of gravity of the group. We calculate the standard deviation σ in the two following hypotheses: spectra 1 and 2 arise respectively from the sites a and b or from the sites b and a. σ is taken as

$$\sigma = \sqrt{\left(\sum (E_{\mathrm{calc}} - E_{\mathrm{obs}})^2 \right) / (30 - 3 - 4)} \quad (13)$$

where the sum runs over the $2 \times (8+7) = 30$ sublevels and we subtract in the denominator 3 because of the three free parameters $\langle r^k \rangle$ and 4 because we have adjusted independently the centres of gravity of the four sets of data. We repeat this procedure for a large number of choices of $\langle r^2 \rangle$, $\langle r^4 \rangle$ and $\langle r^6 \rangle$, in order to obtain the best agreement between calculation and

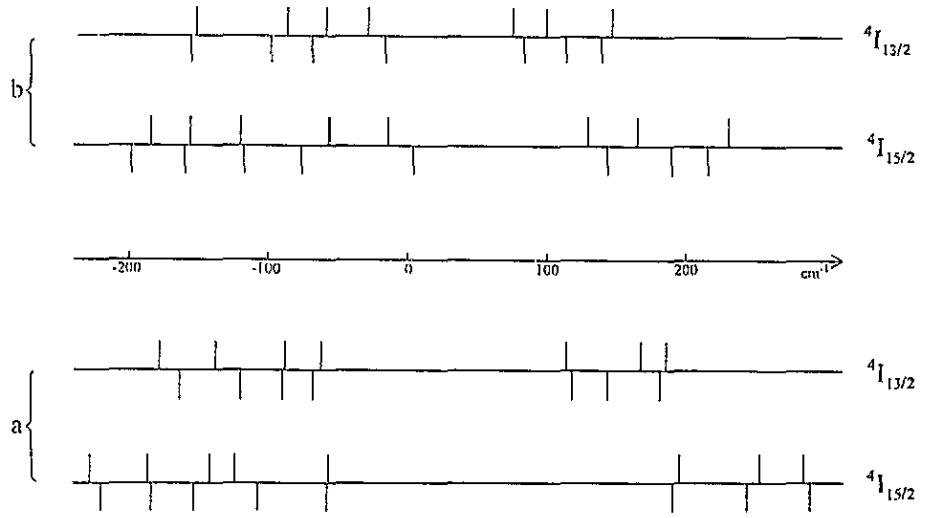

Figure 5. Comparison of observed and calculated crystal field sublevels for $^4I_{15/2}$ and $^4I_{13/2}$ states. Observed and calculated spectra are shown respectively above and under the horizontal lines. (a) Observed spectrum 1 and calculated spectrum for site a; (b) Observed spectrum 2 and calculated spectrum for site b. The four centres of gravity of observed levels have been shifted, in order to coincide with the barycentre of calculated levels (0 cm^{-1}). The values of adjusted parameters are $\langle r^2\rangle = 0.0406$ Å^2, $\langle r^4\rangle = 0.2010$ Å^4 and $\langle r^6\rangle = 0.4359$ Å^6.

Table 5. Results of crystal field calculations. The $\langle r^k\rangle$ are introduced in section 4.1 and σ is defined by equation (13).

	First hypothesis: spectrum 1 corresponds to site a spectrum 2 corresponds to site b	Second hypothesis: spectrum 1 corresponds to site b spectrum 2 corresponds to site a
$\langle r^2\rangle$ (Å^2)	0.0406	0.0522
$\langle r^4\rangle$ (Å^4)	0.2010	0.1683
$\langle r^6\rangle$ (Å^6)	0.4359	0.5365
σ (cm^{-1})	13.8	49.5

experiment. This task is performed with a Fortran program running on an IBM 6151-115 computer.

The results are given in table 5. One remarks that they strongly favour the hypothesis 'spectrum 1 corresponds to site a and spectrum 2 to site b': the standard deviation is more than three times smaller than in the opposite hypothesis (for the best choice of adjustable parameters in each case). The chief reason for this closer fit is that the overall splitting of $^4I_{15/2}$ and of $^4I_{13/2}$ are larger in spectrum 1 than in spectrum 2, and larger in the calculation for site a than for site b. As expected, the values of $\langle r^k\rangle$ parameters have unrealistic values: Freeman and Watson (1962) calculate for 4f electrons of erbium $\langle r^k\rangle = 0.1865$ Å^2, 0.0883 Å^4 and 0.0873 Å^6 for $k = 2, 4$ and 6 respectively. These values are quite different from those listed in table 5. Figure 5 compares observed level schemes 1 and 2 with the best calculation for sites a and b respectively. The agreement is rather good, especially when one considers the simplicity of the present calculation. In particular, the observed separation of sublevels into two groups (both in $^4I_{15/2}$ and in $^4I_{13/2}$) is nicely reproduced,

with the right number of components in each group. A similar energetic separation into two groups is also observed for erbium in other matrices such as YAG (see, for instance, Gruber *et al* 1993), but with a somewhat different aspect: $^4I_{15/2}$ is split into two groups of four sublevels and the group of four sublevels of $^4I_{13/2}$ is energetically above the group of three.

In conclusion, we believe strongly that the spectrum 1 (third column of table 2) arises from crystallographic site a, as defined by columns 2 to 5 of table 1. However, we cannot be completely affirmative because of the crudeness of some of our hypotheses (section 4.1).

Acknowledgments

We thank very much Drs C Borel and Ch Wyon of LETI, Grenoble, who kindly furnished us with the two YSO:Er^{3+} samples we used in all our experiments. We also gratefully acknowledge the help of Professor Ph Labbé and of Dr M Thuau, both of Caen, who helped us to understand the microscopic structure of YSO.

References

Doualan J L, Labbé C, Le Boulanger P, Margerie J, Moncorgé R and Timonen H 1994 *26th EGAS Conf. (Barcelona, 1994)*

Freeman A J and Watson R E 1962 *Phys. Rev.* **127** 2058

Gruber J B, *Quagliano J R, Reid M F, Richardson F S, Hills M E, Seltzer M D, Stevens S B, Morrison C A and* Allik T H 1993 *Phys. Rev.* B **48** 15 561

Judd B R 1957 *Proc. R. Soc.* A **241** 414

——1963 *Operator Techniques in Atomic Spectroscopy* (New York: McGraw-Hill)

Li C 1992 *Thesis* Université Claude-Bernard Lyon I

Li C, Moncorgé R, Souriau J C, Borel C and Wyon Ch 1994 *Opt. Commun* **107** 61

Li C, Wyon C and Moncorgé R 1992 *IEEE J. Quantum Electron.* **QE-28** 1209

Maksimov B A, Ilyukhin V V, Kharitonov Yu A and Belov N V 1970 *Kristallografiya* **15** 926 (Engl. Transl. 1971 *Sov. Phys.–Crystallogr.* **15** 806)

Nielson C W and Koster G F 1963 *Spectroscopic Coefficients for the p^n, d^n and f^n Configurations* (Cambridge, MA: MIT Press)

Pearson W B (ed) 1970 *Structure Reports* vol 35A (Utrecht: Oosthoek, Scheltema and Holkema) p 297

Pinto J F, Georgiou E and Pollock C R 1986 *Opt. Lett.* **11** 519

Rajnak K 1965 *J. Chem. Phys.* **43** 847

Spariosu K, Stultz R D, Camargo M B, Birnbaum M, Montgomery S and Chai B 1994 *Advanced Solid State Lasers Conf. (Salt Lake City, UT, 1994)* (Washington, DC: Optical Society of America)

Wybourne B G 1965 *Spectroscopic Properties of Rare Earths* (New York: Wiley)